

## Horizon Formation and Far-from-Equilibrium Isotropization in a Supersymmetric Yang-Mills Plasma

Paul M. Chesler and Laurence G. Yaffe

*Department of Physics, University of Washington, Seattle, Washington 98195, USA*

(Received 26 February 2009; published 29 May 2009)

Using gauge-gravity duality, we study the creation and evolution of anisotropic, homogeneous strongly coupled  $\mathcal{N} = 4$  supersymmetric Yang-Mills plasma. In the dual gravitational description, this corresponds to horizon formation in a geometry driven to be anisotropic by a time-dependent change in boundary conditions.

DOI: 10.1103/PhysRevLett.102.211601

PACS numbers: 11.25.Tq, 04.70.Dy, 11.10.Wx, 12.38.Mh

*Introduction.*—The realization that the quark-gluon plasma (QGP) produced at RHIC is strongly coupled [1] has prompted much interest in the study of strongly coupled non-Abelian plasmas. Hydrodynamic simulations of heavy ion collisions have demonstrated that the QGP produced at RHIC is well modeled by near-ideal hydrodynamics [2], which is a signature of a strongly coupled system. The success of hydrodynamic modeling of RHIC collisions suggests that the produced plasma locally isotropizes over a time scale  $\tau_{\text{iso}} \lesssim 1 \text{ fm}/c$  [3]. Understanding the dynamics responsible for such rapid isotropization in a far-from-equilibrium non-Abelian plasma is a challenge.

Because of the difficulty in studying real time dynamics in QCD at strong coupling, it is useful to have a toy model where one can study the dynamics of a far-from-equilibrium, strongly coupled non-Abelian plasma in a controlled setting. One such toy model is strongly coupled  $\mathcal{N} = 4$  supersymmetric Yang-Mills (SYM) theory, where one can use gauge-gravity duality to study the theory in the limit of large  $N_c$  and large 't Hooft coupling  $\lambda$ . This has motivated much work devoted to studying various non-equilibrium properties of thermal SYM plasma.

We are interested in exploring the physics of isotropization in far-from-equilibrium non-Abelian plasmas, in the simplest setting which allows complete theoretical control. This leads us to focus on the dynamics of homogeneous, but anisotropic, states in strongly coupled, large  $N_c$  SYM theory. A conceptually simple way to create nonequilibrium states is to turn on time-dependent background fields coupled to operators of interest. To create states in which the stress tensor is anisotropic, it is natural to consider the response of the theory to a time-dependent change in the spatial geometry. For simplicity, we limit attention to geometries which have spatial homogeneity (i.e., translation invariance in all spatial directions), an  $O(2)$  rotation invariance, and a constant spatial volume element. The most general metric satisfying these conditions may be written as

$$ds^2 = -dt^2 + e^{B_0(t)} dx_{\perp}^2 + e^{-2B_0(t)} dx_{\parallel}^2, \quad (1)$$

where  $\mathbf{x}_{\perp} \equiv \{x_1, x_2\}$ .

The function  $B_0(t)$  describes a time-dependent shear in the geometry; neglecting (four-dimensional) gravity,  $B_0(t)$  is a function one is free to choose arbitrarily. We will choose  $B_0(t)$  to be asymptotically constant as  $t \rightarrow \pm\infty$ . We will also choose the initial state to be the SYM vacuum. A time-dependent geometry will do work on the quantum system. Consequently, the state in the distant future will be a nonvacuum state which (when the geometry is once again static) will be indistinguishable from a thermal state. During the evolution, because the metric (1) changes in an anisotropic fashion, the resulting plasma will also be anisotropic with different pressures (i.e., stress tensor eigenvalues) in the longitudinal ( $x_{\parallel}$ ) and transverse ( $\mathbf{x}_{\perp}$ ) directions. Spatial translation invariance implies that no hydrodynamic modes can be excited. Therefore, the non-equilibrium plasma produced by the changing metric (1) provides a nice laboratory to study the relaxation of non-hydrodynamic degrees of freedom in a far-from-equilibrium setting. We choose

$$B_0(t) = \frac{1}{2}c[1 - \tanh(t/\tau)]. \quad (2)$$

For  $c \neq 0$ , this represents a time-dependent rescaling of lengths in transverse directions relative to those in the longitudinal direction, over a period of order  $\tau$ . The lack of any other scale in conformally invariant SYM theory implies that the final state energy density will be  $\mathcal{O}(\tau^{-4})$ . Without loss of generality we measure all quantities in units where  $\tau = 1$ .

*Gravitational description.*—Gauge-gravity duality [4] provides a gravitational description of large  $N_c$  SYM theory in which the 5D dual geometry is governed by Einstein's equations with a cosmological constant. Einstein's equations imply that the boundary metric  $g_{\mu\nu}^B(x)$ , which characterizes the geometry of the spacetime boundary, is dynamically unconstrained. The specification of the boundary metric serves as a boundary condition for

the 5D Einstein equations. This reflects the fact that the dual field theory (residing on the boundary) does not back-react on the boundary geometry, although the boundary geometry influences the field theory dynamics.

We consider a 5D geometry which coincides with AdS<sub>5</sub> in the distant past. This geometry is dual to the SYM vacuum. A time-dependent boundary metric  $g_{\mu\nu}^B(x)$  will create gravitational radiation which propagates from the boundary into the bulk. This infalling gravitational radiation will lead to the formation of a horizon, which acts as an absorber of gravitational radiation—any radiation which passes through the horizon cannot escape back to the boundary. At late times when the boundary geometry is no longer changing, the bulk geometry outside the horizon will relax and asymptotically become static. This is the gravitational description of thermalization in SYM theory.

Diffeomorphism and translation invariance allows one to chose the metric ansatz

$$ds^2 = -Adv^2 + \Sigma^2[e^B dx_{\perp}^2 + e^{-2B} dx_{\parallel}^2] + 2drdv, \quad (3)$$

where  $A$ ,  $B$ , and  $\Sigma$  are all functions of the radial coordinate  $r$  and time  $v$  only. Infalling radial null geodesics have constant values of  $v$  (as well as  $x_{\perp}$  and  $x_{\parallel}$ ). Outgoing radial null geodesics satisfy  $dr/dv = \frac{1}{2}A$ . At the boundary, located at  $r = \infty$ , the coordinate  $v$  coincides with the boundary time  $t$ . The geometry in the bulk at  $v > 0$  corresponds to the causal future of  $t > 0$  on the boundary. The form of the metric (3) is invariant under the residual diffeomorphism  $r \rightarrow r + f(v)$ , where  $f(v)$  is arbitrary.

With a metric of the form (3), Einstein's equations may be reduced to the following set of differential equations:

$$0 = \Sigma(\dot{\Sigma})' + 2\Sigma'\dot{\Sigma} - 2\Sigma^2, \quad (4a)$$

$$0 = \Sigma(\dot{B})' + \frac{3}{2}(\Sigma'\dot{B} + B'\dot{\Sigma}), \quad (4b)$$

$$0 = A'' + 3B'\dot{B} - 12\Sigma'\dot{\Sigma}/\Sigma^2 + 4, \quad (4c)$$

$$0 = \ddot{\Sigma} + \frac{1}{2}(\dot{B}^2\Sigma - A'\dot{\Sigma}), \quad (4d)$$

$$0 = \Sigma'' + \frac{1}{2}B'^2\Sigma, \quad (4e)$$

where, for any function  $h(r, v)$ ,

$$h' \equiv \partial_r h, \quad \dot{h} \equiv \partial_v h + \frac{1}{2}A\partial_r h. \quad (5)$$

Equations (4d) and (4e) are constraint equations; the radial derivative of Eq. (4d) and the time derivative of Eq. (4e) are implied by Eqs. (4a)–(4c).

The above set of differential equations must be solved subject to boundary conditions imposed at  $r = \infty$ . The requisite condition is simply that the boundary metric  $g_{\mu\nu}^B(x)$  coincide with our choice (1) of the 4D geometry. In particular, we must have

$$\lim_{r \rightarrow \infty} \Sigma(r, v)/r \equiv 1, \quad \lim_{r \rightarrow \infty} B(r, v) \equiv B_0(v). \quad (6)$$

One may fix the residual diffeomorphism invariance by demanding that

$$\lim_{r \rightarrow \infty} [A(r, v) - r^2]/r = 0. \quad (7)$$

These boundary conditions, plus initial data satisfying the constraint (4e) on some  $v = \text{const}$  slice, uniquely specify the subsequent evolution of the geometry.

Given a solution to Einstein's equations, the SYM stress tensor is determined by the near-boundary behavior of the 5D metric [5]. If  $S_G$  denotes the gravitational action, then the SYM stress tensor is given by  $T^{\mu\nu}(x) = [2/\sqrt{-g^B(x)}]\delta S_G/\delta g_{\mu\nu}^B(x)$ .

Near the boundary one may solve Einstein's equations with a power series expansion in  $r$ . Specifically,  $A$ ,  $B$ , and  $\Sigma$  have asymptotic expansions of the form

$$A(r, v) = \sum_{n=0} [a_n(v) + \alpha_n(v) \log r] r^{2-n}, \quad (8a)$$

$$B(r, v) = \sum_{n=0} [b_n(v) + \beta_n(v) \log r] r^{-n}, \quad (8b)$$

$$\Sigma(r, v) = \sum_{n=0} [s_n(v) + \sigma_n(v) \log r] r^{1-n}. \quad (8c)$$

The boundary conditions (6) and (7) imply that  $b_0(v) \equiv B_0(v)$ ,  $s_0(v) \equiv 1$ ,  $a_0(v) \equiv 1$ , and  $\alpha_1(v) \equiv 0$ . Substituting the above expansions into Einstein's equations and solving the resulting equations order by order in  $r$ , one finds that there is one undetermined coefficient,  $b_4(v)$ . All other coefficients are determined by the boundary geometry, Einstein's equations, and  $b_4(v)$  [6].

By substituting the above series expansions into the variation of the on shell gravitational action, one may compute the expectation value of the stress tensor in terms of the expansion coefficients. This procedure has been carried out in Ref. [5], so we simply quote the results. In terms of the expansion coefficients, the SYM stress tensor reads

$$T_{\nu}^{\mu} = (N_c^2/2\pi^2) \text{diag}(-\mathcal{E}, \mathcal{P}_{\perp}, \mathcal{P}_{\perp}, \mathcal{P}_{\parallel}), \quad (9)$$

where (with  $b_0^{(k)} \equiv \partial_v^k b_0$ )

$$-\mathcal{E} = \frac{3}{4}a_4 + \frac{1}{256}[3(b_0^{(1)})^4 + 14(b_0^{(2)})^2 - 4b_0^{(1)}b_0^{(3)}], \quad (10a)$$

$$\mathcal{P}_{\perp} = -\frac{1}{4}a_4 + b_4 + \frac{1}{768}[21(b_0^{(1)})^4 - 468(b_0^{(1)})^2b_0^{(2)} + 10(b_0^{(2)})^2 + 4b_0^{(1)}b_0^{(3)} + 64b_0^{(4)}], \quad (10b)$$

$$\mathcal{P}_{\parallel} = -\frac{1}{4}a_4 - 2b_4 + \frac{1}{768}[21(b_0^{(1)})^4 + 936(b_0^{(1)})^2b_0^{(2)} + 10(b_0^{(2)})^2 + 4b_0^{(1)}b_0^{(3)} - 128b_0^{(4)}]. \quad (10c)$$

*Numerics.*—One may solve the Einstein equations (4a)–(4c) for the time derivatives  $\dot{\Sigma}$ ,  $\dot{B}$ , and  $A''$ . Define

$$\Theta(r, v) \equiv \int_r^{\infty} dw [\Sigma(w, v)^3 - h_1(w, v)] - H_1(r, v), \quad (11a)$$

$$\Phi(r, v) \equiv \int_r^{\infty} dw [2\Theta(w, v)B'(w, v)\Sigma(w, v)^{-3/2} - h_2(w, v)] - H_2(r, v), \quad (11b)$$

where  $H_n$  is an indefinite (radial) integral of  $h_n$ ,

$$h_n = H'_n. \quad (12)$$

Then Eqs. (4a)–(4c) are solved by

$$\dot{\Sigma} = -2\Theta\Sigma^{-2}, \quad (13a)$$

$$\dot{B} = -\frac{3}{2}\Phi\Sigma^{-3/2}, \quad (13b)$$

$$A'' = -4 - 24\Theta\Sigma'/\Sigma^{-4} + \frac{9}{2}\Phi B'\Sigma^{-3/2}. \quad (13c)$$

The functions  $h_n(r, \nu)$  are not constrained by Einstein's equations—their presence inside the integrands of Eq. (11) are compensated by the subtraction of their integrals  $H_n(r, \nu)$ . However, since we have chosen the upper limit of integration in Eq. (11) to be  $r = \infty$ , the functions  $h_n(r, \nu)$  must be suitably chosen so that the integrals (11) are convergent. The simplest choice to accomplish this is to set  $h_1(r, \nu)$  equal to the asymptotic expansion of  $\Sigma(r, \nu)^3$  up to order  $1/r^k$ , for some  $k > 1$ , and to set  $h_2(r, \nu)$  equal to the asymptotic expansion of  $2\Theta(r, \nu)B'(r, \nu)/\Sigma(r, \nu)^{3/2}$  up to order  $1/r^k$ . In our numerical solutions reported below, we use  $k \geq 4$ . This choice makes the large  $r$  contribution to the integrals in Eq. (11) quite small. As the coefficients of the series expansions (8) only depend on  $b_0(\nu)$  and  $b_4(\nu)$  and their  $\nu$  derivatives, this choice determines  $h_n(r, \nu)$  in terms of one unknown function  $b_4(\nu)$ .

With the subtraction functions  $h_n$  specified by the aforementioned asymptotic expansions, integrating Eq. (12) fixes the compensating integrals  $H_n$  up to an integration constant which is an arbitrary function of  $\nu$ . Integrating Eq. (13c) for  $A(r, \nu)$  introduces two further ( $\nu$  dependent) constants of integration. The most direct route for fixing these constants of integration is to match the large  $r$  behavior of the expressions (13a) and (13b) and the integrated version of Eq. (13c) to the corresponding expressions obtained from the series expansions (8). This fixes all integration constants in terms of  $b_0$  and  $b_4$ .

Our algorithm for solving the initial value problem with time-dependent boundary conditions is as follows. Given an initial geometry defined by  $B(r, \nu_0)$ , one knows  $b_4(\nu_0)$ . Integrating the constraint equation (4e), with the fully determined asymptotic behavior (8c), yields  $\Sigma(r, \nu_0)$ . From this information, one can compute  $A(r, \nu_0)$  by integrating Eq. (13c). With  $A(r, \nu_0)$ ,  $B(r, \nu_0)$ , and  $\Sigma(r, \nu_0)$  known, one can then compute the time derivative  $\partial_\nu B(r, \nu_0)$  from Eq. (13b) and step forward in time,

$$B(r, \nu_0 + \Delta\nu) \approx B(r, \nu_0) + \partial_\nu B(r, \nu_0)\Delta\nu. \quad (14)$$

Repeating the above process using this updated profile of  $B$  determines  $\Sigma$  and  $A$  at time  $\nu_0 + \Delta\nu$ , from which one computes  $\partial_\nu B$  for the next time step. For an initial geometry corresponding to the SYM vacuum, plus the choice (2) of boundary data, one has

$$B(r, -\infty) = c, \quad \Sigma(r, -\infty) = r, \quad A(r, -\infty) = r^2. \quad (15)$$

An important practical matter is fixing the computation domain in  $r$ —how far into the bulk does one want to compute the geometry? If a horizon forms, then one may excise the geometry inside the horizon as this region is causally disconnected from the geometry outside the horizon. Furthermore, one must excise the geometry to avoid singularities behind horizons [7]. To perform the excision, one first identifies the location of an apparent horizon (an outermost marginally trapped surface) which, if it exists, must lie inside a true horizon [8]. We have chosen to make the incision slightly inside the location of the apparent horizon. For the metric (3), the location  $r_h(\nu)$  of the apparent horizon is given by  $\dot{\Sigma}(r_h(\nu), \nu) = 0$  or, from Eq. (13a),  $\Theta(r_h(\nu), \nu) = 0$ .

*Results and discussion.*—Figure 1 shows a plot of the energy density and transverse and longitudinal pressures produced by the changing boundary geometry (1), with  $c = 2$ . These quantities begin at zero in the distant past when the system is in its vacuum state, and at late times approach thermal equilibrium values given by

$$T_{\text{eq}}^{\mu\nu} = (\pi^2 N_c^2 T^4 / 8) \text{diag}(3, 1, 1, 1), \quad (16)$$

where  $T$  is the final equilibrium temperature. Nonmonotonic behavior is seen when the boundary geometry changes most rapidly around time zero [9].

Figure 2 displays the congruence of outgoing radial null geodesics, for  $c = 2$ . The surface coloring shows  $A/r^2$ . In the SYM vacuum (i.e., at early times) this quantity equals 1, while at late times  $A/r^2 = 1 - (r_h/r)^4$ . Excised from the plot is a region of the geometry behind the apparent horizon. In the SYM vacuum, outgoing geodesics are given by  $1/r + \nu/2 = \text{const}$ , and appear as straight lines in the early part of Fig. 2. In the vicinity of  $\nu = 0$ , when the boundary geometry is changing rapidly and producing infalling gravitational radiation, the geodesic congruence changes dramatically from the zero temperature form to a finite temperature form. As is evident from the figure, at late times some outgoing geodesics do escape to the

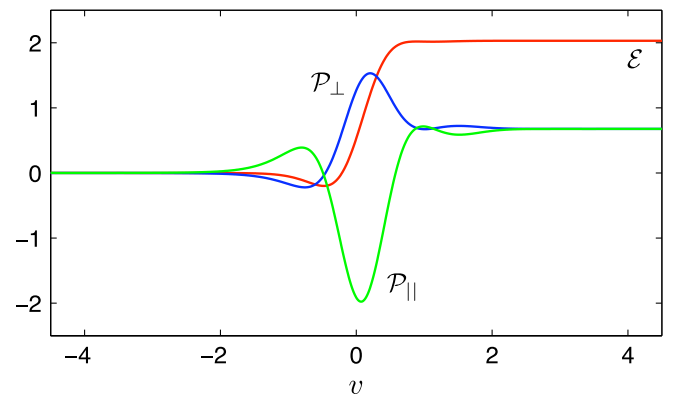


FIG. 1 (color online). Energy density, longitudinal and transverse pressure, all divided by  $N_c^2/2\pi^2$ , as a function of time for  $c = 2$ .

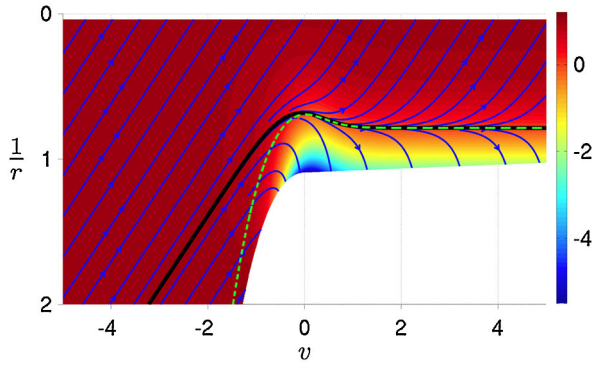


FIG. 2 (color online). The congruence of outgoing radial null geodesics. The surface coloring displays  $A/r^2$ . The excised region is beyond the apparent horizon, which is shown by the dashed green curve. The geodesic shown as a solid black line is the event horizon; it separates geodesics which escape to the boundary from those which cannot escape.

boundary, while others fall into the bulk and never escape. Separating the “escaping” and “plunging” geodesics is one geodesic which does neither—this geodesic, shown as the black line in Fig. 2, defines the true event horizon of the geometry.

Figure 3 plots the area of the apparent and true event horizons, again for  $c = 2$ . Nearly all growth of the apparent horizon area occurs in the interval  $-2 < v < 0$ , during which the boundary geometry is changing rapidly. In contrast, the area of the true horizon grows in the distant past long before the boundary geometry is significantly perturbed. This is a reflection of the global nature of event horizons—the location of the event horizon depends on the entire history of the geometry. It has been argued [11] that it is the area element of the apparent horizon, pulled back to the boundary along  $v = \text{const}$  infalling null geodesics, which should be identified with the entropy density (times  $4G_N$ ) in the dual field theory.

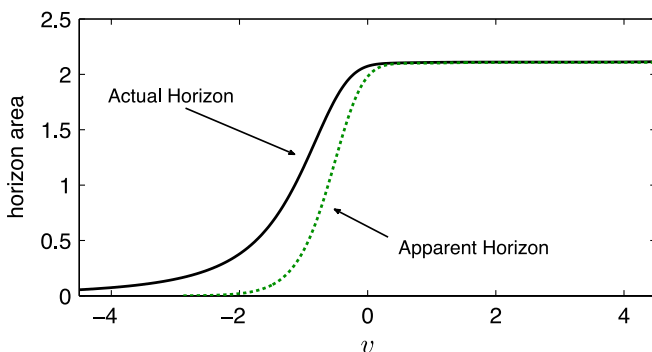


FIG. 3 (color online). Area elements of the true event horizon and the apparent horizon as a function of time.

TABLE I. Final equilibrium temperature  $T$  and isotropization time  $\tau_{\text{iso}}$  (in units of  $T^{-1}$  or  $\tau$ ), for various values of  $c$ . The isotropization time  $\tau_{\text{iso}}$  is the time at which the pressures deviate from their equilibrium values by less than 10%.

$ c $	1	1.5	2	2.5	3	3.5	4
$\tau T$	0.23	0.31	0.41	0.52	0.65	0.79	0.94
$\tau_{\text{iso}} T$	0.67	0.68	0.71	0.92	1.2	1.5	1.8
$\tau_{\text{iso}}/\tau$	3.0	2.2	1.7	1.8	1.8	1.9	1.9

Table I shows, for various values of  $c$ , the final equilibrium temperature  $T$  and a measure of the isotropization time  $\tau_{\text{iso}}$ . (These quantities only depend on  $|c|$ .) We define  $\tau_{\text{iso}}$  as the time when the transverse and longitudinal pressures equal their final values to within 10%. When  $|c| \geq 2$ , we find that  $\tau_{\text{iso}} \approx 2\tau$ , while for  $|c| \leq 2$ ,  $\tau_{\text{iso}} \approx 0.7/T$ . Since  $\tau_{\text{iso}}$  is only a few times longer than the time scale  $\tau$  over which the boundary geometry (1) is changing, this measure of isotropization time should best be viewed as an upper bound on isotropization times associated with plasma dynamics alone. Nevertheless, it is interesting to note that  $\tau_{\text{iso}} \approx 0.7/T$  corresponds to a time of  $\frac{1}{2} \text{ fm}/c$  when  $T = 350 \text{ MeV}$ , similar to estimates of thermalization times inferred from hydrodynamic modeling of RHIC collisions [3].

This work was supported in part by the U.S. Department of Energy under Grant No. DE-FG02-96ER40956.

- [1] E. V. Shuryak, Nucl. Phys. **A750**, 64 (2005).
- [2] M. Luzum and P. Romatschke, Phys. Rev. C **78**, 034915 (2008).
- [3] U. W. Heinz, AIP Conf. Proc. **739**, 163 (2004).
- [4] J. M. Maldacena, Int. J. Theor. Phys. **38**, 1113 (1999).
- [5] S. de Haro, S. N. Solodukhin, and K. Skenderis, Commun. Math. Phys. **217**, 595 (2001).
- [6] The coefficient  $a_4$  is determined by a first-order ordinary differential equation, which can be obtained from the condition that the SYM stress tensor be covariantly conserved. All other coefficients are determined algebraically from  $b_0(v)$ ,  $b_4(v)$ ,  $a_4(v)$ , and their  $v$  derivatives.
- [7] P. Anninos, G. Daues, J. Masso, E. Seidel, and W.-M. Suen, Phys. Rev. D **51**, 5562 (1995).
- [8] R. M. Wald, *General Relativity* (University of Chicago, Chicago, 1984), p. 491.
- [9] Nonmonotonicity is unsurprising. Late time response for  $|c| \ll 1$  is dominated by the lowest quasinormal mode whose frequency is complex,  $\omega_{\text{QNM}} = (\pm 9.8 - 8.7i)T$  [10].
- [10] A. O. Starinets, Phys. Rev. D **66**, 124013 (2002).
- [11] V. E. Hubeny, M. Rangamani, and T. Takayanagi, J. High Energy Phys. **07** (2007) 062.